Vol 17 No 4, April 2008
1674-1056/2008/17(04)/1371-06

Chinese Physics B

© 2008 Chin. Phys. Soc.
and IOP Publishing Ltd

Magnetic properties of Mn-doped ZnO diluted magnetic semiconductors*

Liu Xue-Chao(刘学超)[a)b)], Zhang Hua-Wei(张华伟)[a)b)],
Zhang Tao(张 涛)[a)], Chen Bo-Yuan(陈博源)[a)b)],
Chen Zhi-Zhan(陈之战)[a)†], Song Li-Xin(宋力昕)[a)], and Shi Er-Wei(施尔畏)[a)]

[a)] *Shanghai Institute of Ceramics, Chinese Academy of Sciences, Shanghai* 200050, *China*
[b)] *Graduate School of the Chinese Academy of Sciences, Beijing* 100049, *China*

(Received 12 July 2007; revised manuscript received 17 October 2007)

A series of Mn-doped ZnO films have been prepared in different sputtering plasmas by using the inductively coupled plasma enhanced physical vapour deposition. The films show paramagnetic behaviour when they are deposited in an argon plasma. The Hall measurement indicates that ferromagnetism cannot be realized by increasing the electron concentration. However, the room-temperature ferromagnetism is obtained when the films are deposited in a mixed argon-nitrogen plasma. The first-principles calculations reveal that antiferromagnetic ordering is favoured in the case of the substitution of Mn^{2+} for Zn^{2+} without additional acceptor doping. The substitution of N for O (N_O^-) is necessary to induce ferromagnetic couplings in the Zn-Mn-O system. The hybridization between N 2p and Mn 3d provides an empty orbit around the Fermi level. The hopping of Mn 3d electrons through the empty orbit can induce the ferromagnetic coupling. The ferromagnetism in the N-doped Zn-Mn-O system possibly originates from the charge transfer between Mn^{2+} and Mn^{3+} via N_O^-. The key factor is the empty orbit provided by substituting N for O, rather than the conductivity type or the carrier concentration.

Keywords: Mn-doped ZnO, diluted magnetic semiconductors, first-principle calculations
PACC: 7115A, 7550P, 7000

1. Introduction

Diluted magnetic semiconductor (DMS) is one of the frontier topics in condensed matter physics due to its potential application in spintronic devices. Transition metals (TMs) doped ZnO has been extensively studied. Room-temperature ferromagnetism in Mn-doped ZnO was initially predicted by Dietl *et al*,[1] Sato and Yoshida,[2] and Kuang *et al.*[3] However, the experiments show diverse magnetic properties from paramagnetism, spin-glass and antiferromagnetism to ferromagnetism at low temperatures or even at high temperatures.[4−9] The origin of ferromagnetism is still controversial, which is attributed to either intrinsic or extrinsic properties of DMS.[10−12] The key issue in the Zn-Mn-O system is whether the hole is absolutely necessary to stabilize ferromagnetic couplings. Dietl *et al*[1] predicted above-room-temperature ferromagnetism in Mn-doped ZnO with a carrier (hole) concentration of $3.5 \times 10^{20}\,\mathrm{cm}^{-3}$ based on the mean-field Zener model. Sato and Yoshida[2] proposed double-exchange mechanism for the carrier induced ferromagnetism in TM-doped ZnO. The ferromagnetism could be enhanced by doping electrons into Fe-, Co-, or Ni-doped ZnO. On the other hand, the stability of ferromagnetism was stabilized by doping holes into Mn-doped ZnO.[2] The first-principles calculations revealed that the doping of acceptor elements, which could be introduced by substituting N for O in ZnO, was crucial to inducing the ferromagnetic coupling.[13−15] Recently, Coey *et al*[16] proposed that the ferromagnetic coupling in oxide-based DMS be mediated by shallow donor electrons through forming bound magnetic polarons (BMP). Experimentally, several research groups have found the room-temperature ferromagnetism in $Zn_{1-x}Mn_xO$: N films with an n-type conductivity.[17−19] However, Kittilstved *et al*[20] demonstrated that the ferromagnetism in Mn-doped ZnO was intimately related to the electronic structure of Mn ions and could be realized only through hole-inducing charge transfer process. Rubi *et al*[21] found that the ferromagnetism in Mn-doped

*Project supported by the Shanghai Nanotechnology Promotion Center (Grant No 0452nm071) and the National Natural Science Foundation of China (Grant Nos 50702071 and 50772122).
†Corresponding author. E-mail: zzchen@mail.sic.ac.cn

ZnO could be obtained by low-temperature annealing in N_2. Ramachandran *et al*[17] reported that the ferromagnetism in the as-deposited $Zn_{1-x}Mn_xO$ ($x = 0.01$–0.1) films disappeared during high temperature annealing in an excess oxygen atmosphere.The above theoretical and experimental results indicate that the origin of ferromagnetism in the Zn–Mn–O system is still unclear.

In this paper, we study the electronic structure and magnetic properties of Zn–Mn–O system through calculation and experiment. In order to investigate the influence of donor and acceptor dopings, Mn-doped ZnO films are prepared with different dopants. We find that the ferromagnetism can be easily obtained by N-doping, no matter what type of conductivity it is.

2. Experimental and computational details

The Mn-doped ZnO films were prepared by inductively coupled plasma enhanced physical vapour deposition (ICP-PVD).[22] The $Zn_{0.96}Mn_{0.04}O$ and $Zn_{0.95}Mn_{0.04}Al_{0.01}O$ ceramic targets were fabricated by using the standard solid-state reaction method. The procedure is briefed below. A prescribed quantity of ZnO (99.99%), MnO (99.99%) and Al_2O_3 (99.99%) powders were mixed, first compressed under 70 MPa in a stainless steel mould, and then compressed under 300 MPa in an oil compression system. The corresponding targets were sintered at 1273 K for 24 h in air and finally quenched to room temperature.[23] They were doped by a few percent aluminium to investigate the effect of donor doping. The base pressure and sputtering pressure were 5×10^{-4} and 1 Pa, respectively. The DC sputtering power was maintained at 100 W with a net power of 25 W applied to rf coil. The Si (100) and quartz glass substrates (for Hall measurement) were kept at 673 K during sputtering. The $Zn_{0.96}Mn_{0.04}O$ (ZMO) and $Zn_{0.95}Mn_{0.04}Al_{0.01}O$ (ZMAO) films were deposited in an argon plasma. A mixed argon-nitrogen plasma (with a flux ratio of 2:1) was also used for sputtering $Zn_{0.96}Mn_{0.04}O$ (ZMO: N) and $Zn_{0.95}Mn_{0.04}Al_{0.01}O$ (ZMAO: N) films in order to investigate the effect of acceptor doping. Samples studied here were of homogeneous wurtzite structure. No detectable phases corresponding to the manganese oxides or the manganese nitride clusters were found by x-ray diffraction and high-resolution transmission electron microscopy. Extended x-ray absorption fine structure indicated that Mn^{2+} ions were substituted for the Zn^{2+} ions in ZnO. Raman scattering experiment revealed that the O^{2-} ions were partially substituted by N when the films were deposited in a mixed argon-nitrogen plasma. The quality characterizations were described elsewhere. In this paper, we focused on the electrical and magnetic properties. Four-point Van der Pauw Hall measurement (LakeShore Hall measurement system, 7704A) was carried out to investigate the electrical properties at room temperature. The magnetic properties were investigated by using a superconducting quantum interference device (SQUID, MPMS XL-7). The first-principles calculations based on the density functional theory and local spin density approximation were carried out to investigate the electronic structure and magnetic properties.[24,25] A periodic $3\times3\times3$ wurtzite supercell containing 108 atoms in a unit cell was used. Two Zn atoms were substituted by Mn atoms, which gave a Mn doping concentration of about 4%. The ionic coordinates and structure relax were fully optimized by using the conjugate gradient technique. The total energies, forces, and geometry were optimized by using a plane wave basis set with the projector augmented plane wave method.[26] The generalized gradient approximation for exchange and correlation was implemented in the Vienna *ab initio* simulation package (VASP). We used a well-converged energy of cutoff of 450 eV for the plane-wave expansion of the projector augmented waves. For the summation of charge densities over a Brillouin zone, a $6\times4\times2$ Monkhorst-Pack mesh centred at G-centre, as k-point, was used.

3. Results and discussion

Figure 1 shows the curve for magnetization versus magnetic field (M–H) of the as-deposited films. Diamagnetic contribution from the Si substrate was subtracted from the corresponding hysteresis curves. The hysteresis curve of ZMO sample is linear with a zero coercive field (H_c). It is a typical behaviour of paramagnetic ordering. By doping with a few percent Al, the ZMAO sample has no significant change in magnetic property. However, the M–H curve of ZMO: N sample clearly shows a hysteresis loop with an H_c of 52 Oe(1Oe=80 A/m) and a saturation mag-

netization (M_s) of 0.18 μ_B/Mn. It is a typical ferromagnetic behaviour. For the ZMAO: N sample, room-temperature ferromagnetic behaviour is still prominent. The H_c and M_s are 80 Oe(1Oe=80 A/m) and 0.28 μ_B/Mn, respectively. Table 1 shows the Hall measurement results. Both ZMO and ZMAO films show n-type conductivity and their electron concentrations are $6.13 \times 10^{17}\,cm^{-3}$ and $6.30 \times 10^{20}\,cm^{-3}$, respectively. When the films were deposited in a mixed argon-nitrogen plasma, ZMAO: N film still shows the n-type conductivity with an electron concentration of $2.00 \times 10^{19}\,cm^{-3}$. However, ZMO: N films exhibit p-type conductivity with a hole concentration of $4.74 \times 10^{15}\,cm^{-3}$. Figure 2 shows the value of Hall resistance (ρ_{xy}) for ZMO and ZMO: N samples at room temperature. The ρ_{xy} in ferromagnetic materials is expressed as a sum of the ordinary and the anomalous Hall terms, i. e. $\rho_{xy} = R_0 H + R_s M$, where R_0 is the ordinary anomalous Hall term, H is the applied magnetic field, R_s is the anomalous Hall coefficient, and M is the magnetization. For a nonferromagnetic ZMO film, the $\rho_{xy}(H)$ is linear in a range from −1280 to 1280 kA/m. The negative slope implies that the charge carriers are of n-type and the ordinary Hall resistance is dominant in the whole magnetic field. In the case of ZMO: N sample, the $\rho_{xy}(H)$ is also almost linear, except at low magnetic fields. The anomalous Hall effect which is proportional to the magnetization, is dominant at lower magnetic fields. Above about 500 Oe, the $\rho_{xy}(H)$ is linear and has a positive slope, implying that the p-type charge carrier is present in the films. The Hall measurements and magnetic properties indicate that the ferromagnetism cannot be enhanced by increasing the electron concentration. It can be easily realized by doping with nitrogen, no matter what type of conductivity it is.

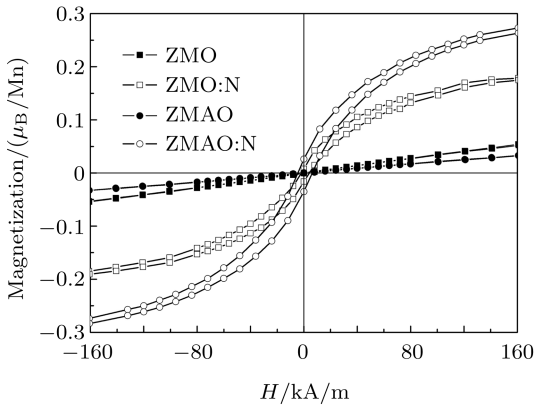


Fig.1. Magnetization hysteresis curves of ZMO, ZMAO, ZMO: N and ZMAO: N films at 300 K.

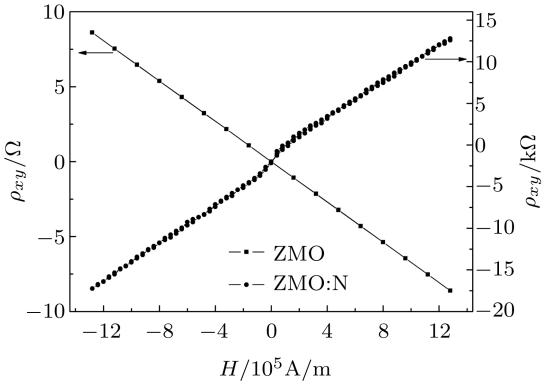


Fig.2. The dependences of Hall resistance on the magnetic field of ZMO and ZMO: N samples.

Table 1. Electrical properties of ZMO, ZMAO, ZMO: N and ZMAO: N films at 300 K.

Sample	Bulk Resistivity/Ω·cm	Mobility/(cm^2/V·S)	Bulk N/cm^{-3}	Type
ZMO	7.42	13.73	6.13×10^{17}	n
ZMAO	7.42×10^{-3}	1.335	6.30×10^{20}	n
ZMO: N	6.79×10^{3}	1.938	4.74×10^{15}	p
ZMAO: N	3.06×10^{-1}	1.022	2.00×10^{19}	n

We have investigated the electronic structure and magnetic properties of Mn-doped and (Mn, N)-codoped ZnO by performing the first-principles calculations. In the Mn-doped ZnO case, the distance between two doped Mn atoms is considered to be the separation from the nearest neighbour to furthest neighbour. One Mn atom is fixed at site 0. The other Mn atom is removed from site 1 to site 10 as shown in Fig.3. In each configuration, the relative energies of ferromagnetic (FM) and antiferromagnetic (AFM) orderings are calculated. The energy difference ($\Delta E = E_{FM} - E_{AFM}$) between FM and AFM orderings is used as an indicator of the magnetic stability. Stable room-temperature ferromagnetism should

be achieved for $\Delta E < -30$ meV when the thermal energy $k_{\rm B}T$ is taken into consideration. The ΔE versus

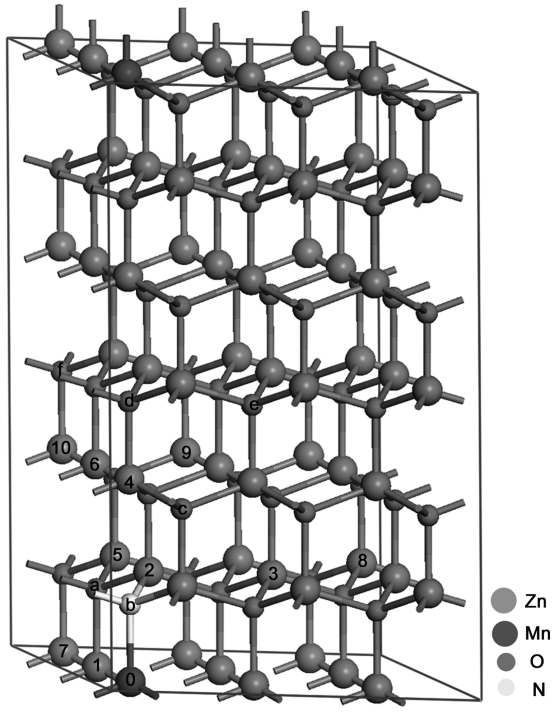


Fig.3. Wurzite Mn-doped ZnO supercell ($3\times3\times3$), where large grey, large black, small black, and small grey spheres represent Zn, Mn, O and N ions, respectively. Different configurations are marked by numbers 1 to10 and letters a to f.

configuration is shown in Fig.4(a). It can be seen that ΔE decreases obviously as the distance between Mn atoms increases. For configurations 1 and 2, the values of ΔE are 45 and 78 meV, respectively. This indicates that the antiferromagnetic ordering is preferable. The absolute value of ΔE is smaller than 30 meV in the other configurations, implying that the interaction between the doped Mn ions is very weak. Neither FM states nor AMF states are stable in these cases. The system gives preference to paramagnetism due to the doped magnetic Mn ions being isolated. Two Mn atoms are separated by one oxygen atom in configuration 2. The largest ΔE reveals the strongest antiferromagnetic coupling between the doped Mn atoms. Therefore, we substitute N for O site in this configuration. Six configurations are also illustrated. (The O sites are labelled with letters a–f) as shown in Fig.3. The calculated values of ΔE is shown in Fig.4(b). The value of ΔE for configuration b is -0.325 eV, which indicates a distinct change from antiferromagnetic ordering to ferromagnetic ordering after doping nitrogen. In the other configurations, the values of ΔE are positive, which means that the antiferromagnetic ordering is a basic state. It can be found that the value of ΔE is very large after introducing nitrogen. The reason may be that the total energy is increased due to the changes in geometric configuration, structural relax, etc. The N atom is located very far from the doped Mn atoms as shown in configurations d, e and f. The AFM state is preferable to other state due to the antiferromagnetic coupling between the doped Mn via O. The ferromagnetic interaction may be very weak because of a large distance between N and Mn atoms. Figure 5 shows the calculated Mn 3d projected local densities of states (PDOS) of configuration 2 (upper panel). The Mn 3d and the N 2p PDOS of configuration b are shown in the bottom panel. In the upper panel, the Fermi energy lies in a region of vanishing electron density. That means that the hybridization

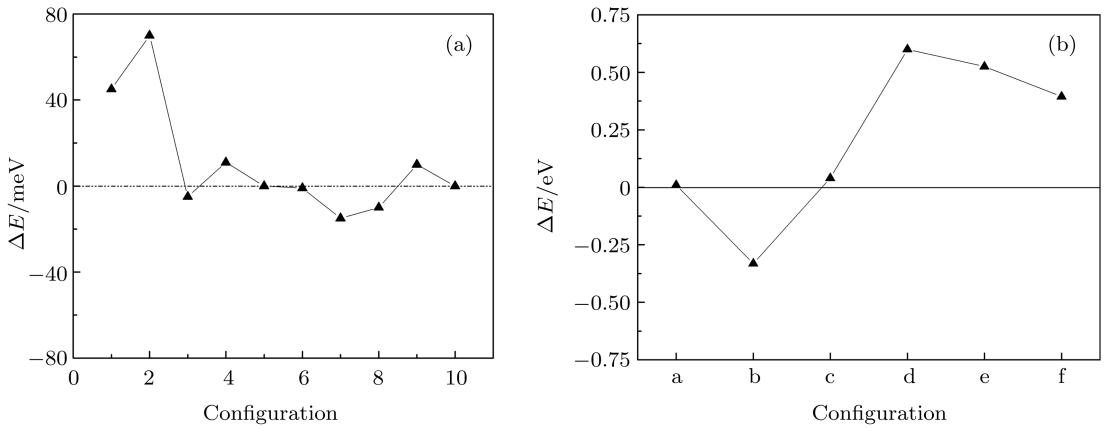


Fig.4. The total energy differences ($\Delta E = E_{\rm FM} - E_{\rm AFM}$) between the ferromagnetic and antiferromagnetic states per Mn ion as a function of the substitution sites, where (a) Mn is substituted for Zn atoms in different configurations and (b) N is substituted for O atoms in Zn–Mn–O system with Mn site in configuration 2.

between O 2p and Mn 3d does not bring in any carriers. In the bottom panel, the N 2p PDOS is plotted in shadow. The Fermi level passes through the spin-up density states, while the spin-down states make no contributions to the DOS. The overlap between N 2p and Mn 3d orbits in the spin-up band result in spin-up DOS around the Fermi level. It is an empty orbit formed by the hybridization between N 2p and Mn 3d. The empty orbit provides the possibility of charge transfer between the Mn 3d and the N 2p.

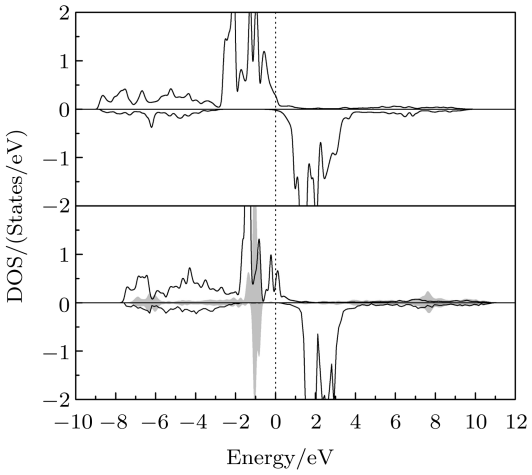


Fig.5. Mn 3d-projected density of states for electrons with up and down spins in configuration 2 (upper panel), and N 2p- (in shadow) and Mn 3d- (solid line) projected density of states for electrons with up and down spins in configuration b (bottom panel).

For the Zn–Mn–O system, the ferromagnetism has been predicted by introducing additional carriers (hole) at high concentrations. In our experiment, both ZMO and ZMAO films do not show any ferromagnetic behaviours. This indicates that the ferromagnetic coupling cannot be realized by doping donors. It is consistent with Sato's and Dietl's theory and most of experimental results.[1,2,5−7] The magnetic properties change dramatically when N is introduced. The ZMO: N films show the p-type conductivity and exhibit the room-temperature ferromagnetism. However, the ZMAO: N films still show room-temperature ferromagnetism with the n-type conductivity. The ferromagnetic behaviours in n-type $Zn_{1-x}Mn_xO$ films are also found in Refs.[17–19] Why can the ferromagnetism come into being in both n-type and p-type Zn-Mn-O system? This question can be answered by the calculation results. The two Mn atoms are separated by one O atom in configuration 2. The antiferromagnetic super-exchange is favoured in energy because no additional carrier is introduced through the substitution of Mn^{2+} for Zn^{2+}.[27,28] This is revealed by calculating the total FM and AFM energies. When the O atom which separates two Mn atoms is substituted by N (N_O^-), N_O^- has one less-occupied p-orbit, which tends to capture one spin electron. The 3d orbit of Mn^{2+} is half-filled with five spin electrons. The hybridization between N 2p and Mn 3d orbits results in the charge transfer through double-exchange mechanism, which means that the Mn^{2+} tends to give an electron to N_O^- (Mn^{2+}- e $\rightarrow$ Mn^{3+}).[20] In order to investigate the effect of the Mn–N distance on ferromagnetic coupling stability, we investigate the total energies for different N sites from a to f. It turns out that the total energy of configuration b is higher than those of other configurations. This implies that the electron hopping to the empty orbit needs a certain amount of energy, since the Fermi level is situated in a spin-up region. The N 2p spin electron at the top of the valency band and the localized Mn 3d spin electrons in the conduction band make Mn^{2+} and Mn^{3+} parallel. The charge transfer Mn^{2+}- e $\rightarrow$ Mn^{3+} can explain why (Mn, N)-codoped ZnO exhibits ferromagnetism even though with n-type conductivity.[20] The crucial factor is not the carrier concentration, but the charge transfer through the empty orbit provided by substituting N for O. That is why ZMO and ZMAO samples do not exhibit ferromagnetic behaviours. The antiferromagnetic coupling is dominant in the case of lacking empty orbit. However, for the ZMO: N and ZMAO: N samples, obvious ferromagnetism is observed even though ZMAO: N shows the n-type conductivity. The key role in inducing ferromagnetism in the Zn–Mn–O system is played by the empty orbit, rather than the conductivity type or the carrier concentration.

4. Conclusions

A series of Mn-doped ZnO films have been prepared by using inductively coupled plasma enhanced physical vapour deposition. Room-temperature ferromagnetism is obtained in Mn-doped ZnO films by doping with nitrogen. The electronic structure and total energy are calculated by the first-principles calculations. Antiferromagnetic ordering in Mn-doped ZnO is favoured in energy. By codoping with nitrogen, the hybridization between N 2p and Mn 3d pro-

vides an empty spin orbit around the Fermi level. The hopping of Mn 3d electrons through the empty orbit can induce the ferromagnetic ordering. The charge transfer between Mn^{2+} and Mn^{3+} may be the origin of ferromagnetism. The key factor is played by the empty orbit, rather than the conductivity type or the carrier concentration.

References

[1] Dietl T, Ohno H, Matsukura F, Cibert J and Ferrand D 2000 *Science* **287** 1019

[2] Sato K and Yoshida H K 2001 *Jpn. J. Appl. Phys.* **40** L334

[3] Kuang A L, Liu X C, Lu Z L, Ren S K, Liu C Y, Zhang F M and Du Y W 2005 *Acta Phys. Sin.* **54** 2934 (in Chinese)

[4] Luo J, Liang J K, Liu Q L, Liu F S, Zhang Y, Sun B J and Rao G H 2005 *J. Appl. Phys.* **97** 086106

[5] Lawes G, Risbud A R, Ramirez A P and Seshadri R 2005 *Phys. Rev.* B **71** 045201

[6] Zhang J, Skomski R and Sellmyer D J 2005 *J. Appl. Phys.* **97** 10D303

[7] Xu H Y, Liu Y C, Xu C S, Liu Y and Shao C L 2006 *J. Chem. Phys.* **124** 074707

[8] Sharma P, Gupta A, Rao K V, Frank J O, Renu S, Rajeev A, Osorio J M, Johansson B and Gehring G A 2003 *Nat. Mater.* **2** 673

[9] Chen W, Zhao L F, Wang Y Q, Miao J H, Liu S, Xia Z C and Yuan S L 2005 *Appl. Phys. Lett.* **87** 042507

[10] Zhang H W, Shi E W, Chen Z Z, Liu X C and Xiao B 2006 *J. Phys.: Condens. Matter* **18** L477

[11] Lusan D, Sanyal B and Eriksson O 2007 *J. Appl. Phys.* **101** 09H101

[12] Mofor A C, Shaer A E, Bakin A and Waag A 2005 *Appl. Phys. Lett.* **87** 062501

[13] Wang Q, Sun Q, Rao B K and Jena P 2004 *Phys. Rev.* B **69** 233310

[14] Wang Q, Sun Q and Jena P 2004 *Phys. Rev.* B **70** 052408

[15] Gopal P and Spaldin N A 2006 *Phys. Rev.* B **74** 094418

[16] Coey J M D, Venkatesan M and Fitzgerald C B 2005 *Nat. Mater.* **4** 173

[17] Ramachandran S, Narayan J and Prater J T 2006 *Appl. Phys. Lett.* **88** 242503

[18] Xu H Y, Liu Y C, Xu C S, Liu Y X, Shao C L and Mu R 2006 *Appl. Phys. Lett.* **88** 242502

[19] Heo Y W, Ivill M P, Ip K, Norton D P, Pearton S J, Kelly J G, Rairigh R, Hebard A F and Steiner T 2004 *Appl. Phys. Lett.* **84** 2292

[20] Kittilstved K R, Liu W and Gamelin D R 2006 *Nat. Mater.* **5** 291

[21] Rubi D, Fontcuberta J, Calleja A, Aragones L, Capdevila X G and Segarra M 2007 *Phys. Rev.* B **75** 155322

[22] Zhao H Y, Fan Q L, Song L X, Zhang T, Shi E W and Hu X F 2006 *Appl. Surf. Sci.* **252** 3065

[23] Liu X C, Shi E W, Chen Z Z, Zhang H W and Song L X 2006 *Acta Phys. Sin.* **55** 2557 (in Chinese)

[24] Li R Q, Lin Q B, Zeng Y Z and Zhu X Z 2006 *Acta Phys. Sin.* **55** 873 (in Chinese)

[25] Ouyang C Y, Xiong Z H, Ouyang Q Z, Liu G D, Ye Z Q and Lei M S 2006 *Chin. Phys.* **15** 1585

[26] Bloechl P E 1994 *Phys. Rev.* B **50** 17953

[27] Sato K and Yoshida H K 2000 *Jpn. J. Appl. Phys.* **39** L555

[28] Sato K and Yoshida H K 2002 *Semicond. Sci. Technol.* **17** 367